Behavior of Rigid Circular Shallow Foundations on Geogrid-Reinforced Sand

Danny José Useche Infante

GIGEF Research Group, PhD Student, Fellow CONICET, Department of Civil Engineering, National Technological University (UTN), the Regional Faculty of Córdoba (Argentina)
e-mail: djusechei@gmail.com

Gonzalo Martin Aiassa Martinez

GIGEF Research Group, Professor of Department of Civil Engineering, National Technological University (UTN), the Regional Faculty of Córdoba (Argentina)
e-mail: gaiassa@scdt.frc.utn.edu.ar

Pedro Ariel Arrúa

GIGEF Research Group, Professor of Department of Civil Engineering, National Technological University (UTN), the Regional Faculty of Córdoba (Argentina)
e-mail: arruapedro@yahoo.com.ar

Marcelo Eberhardt

GIGEF Research Group, Professor of Department of Civil Engineering, National Technological University (UTN), the Regional Faculty of Córdoba (Argentina)
e-mail: meberhardt@civil.frc.utn.edu.ar

ABSTRACT

This paper presents the effect of two types of geogrid inclusion on the bearing capacity of a rigid circular footing resting on sand. The improvement achieved with uniaxial and biaxial geogrids is compared. Load tests were performed for a broad series of conditions, including unreinforced cases, was tested by varying variables such as geogrid type, number of geogrid layers, depth to topmost layer of geogrid and the case when the geogrid is anchored to the test mold. The results were then analyzed to find both qualitative and quantitative relationships between the bearing capacity and the geogrid variables. The results of the investigation indicate that both, the settlement and the bearing capacity, of circular footing resting on sand, can be enhanced by the presence of geogrid layers. The improvement in stress-strain behavior of the geogrid-reinforced sand was found to be strongly dependent on the number of geogrid layers, vertical distance between the base of the foundation and the first layer of geogrid and the tensile strength of geogrid reinforcement.

KEYWORDS: Shallow foundations, geogrid, reinforced soil, bearing capacity ratio, settlement.

INTRODUCTION

The subject of reinforcing soil beneath footings has gained considerable attention in the past few years. Several experimental studies were conducted to evaluate the bearing capacity of footings on reinforced soil, some of these studies include series of laboratory scale load tests on model footings on reinforced soil contained in tanks (Wasti and bütün 1996, Adams and Collin 1997, Das *et al*. 1998, Kotake *et al*. 2001, DeMerchant *et al*. 2002, Patra *et al*. 2005, Basudhar *et al*. 2007, Latha and Somwanshi 2009, Phanikumar *et al*. 2009, Moghaddas Tafreshi and Dawson 2012, Abu-Farsakh *et al*. 2013, Marto *et al*. 2013, Yadu and Tripathi 2013, Azzam and Nasr 2014, Dixit and Patil 2014). Primarily, control parameters in these tests were: the location of the top layer of the reinforcement measured from the bottom of the foundation, the depth of reinforcement, the number of reinforcement layers, the length of each reinforcement layer and vertical separation between layers of geosynthetic. These investigations have concluded that, the inclusion of one or more geosynthetic layers as reinforcement in a granular soil mass beneath shallow footings, is an effective means of reducing settlements and increasing the load bearing capacity.

Bergado *et al*. (2001) conducted an investigation with a modified Laboratory California Bearing Ratio (CBR) device to characterize the behavior of soil-geotextile system and the mechanism of reinforced. Yetimoglu *et al*. (2005) performed CBR test on sand fills reinforced with randomly distributed discrete fibers overlying soft clay and reported that adding fiber inclusions in sand fill resulted in an appreciable increase in the peak piston load. The effect of the inclusion of geogrids in granular road base material by CBR tests was studied by Duncan-Williams and Attoh-Okine (2008). Naeini and Mirzakhanlari (2008) performed CBR test on nonwoven needle-punched geotextile combines with the granular soils with different grading and the comparison between bearing capacity of soil with and without geotextile reinforcement under axisymmetric loading condition were investigated. Senthil Kumar and Rajkumar (2012) studied the effect of woven and non-woven geotextiles on the CBR strength of the aggregate – soil system, considering the clay with high compressibility as soft subgrade. These investigations concluded that the inclusion of reinforcing geosynthetic materials in soils improves the CBR and therefore the strength of soils. Some results of the stress-strain behavior of uniaxial geogrid-reinforced sand of Córdoba were reported in Useche Infante *et al*. (2015), these results are part of the research presented in this paper and are discussed in detail later.

In the present study, the bearing capacity and settlement behavior of circular footings on reinforced sand of Córdoba with geogrid layers are investigated using a small-scale laboratory tests. Two series of experiments with different types of geosynthetic included were conducted with the aim to compare the effect of the inclusion of two types of geogrid. Samples were tested with and without geogrid included in the soil mass and geogrid samples anchored to the test mold. These samples with geogrid anchored to the test mold was conducted in order to reproduce the condition in which the geogrid is pressed by compacted ground and a tension force occurs when the geogrid deforms by the application of loads. Finally, the influence of some variables of the soil-geogrid system in the stress-strain behavior of reinforced soil is investigated. The variables studied are: distance between the base of the foundation and the first layer of geogrid (u) and the number of geogrid layers (N).

LABORATORY TESTS

Materials

In the laboratory tests two different reinforcement type and compacted sand was used. The necessary details of the materials used in the tests are presented as follows.

Natural Sand

The soil used in the study is natural sand of Córdoba Argentina. This soil is commonly utilized in shallow foundations of structures and embankments. The particle size distribution was characterized using the dry sieving method and the results are shown in Figure 1. The sand is classified by the USCS system as SW (well graded sand) with uniformity coefficient C_u=8.57, curvature coefficient C_c=1.47, the mean grain size D_{50}=1.32 mm, size D_{60}=1.63 mm, size D_{30}=0.67 mm and size D_{10}=0.19 mm. Samples for the laboratory test were compacted according to ASTM D 698 (Method C), compaction details of each specimen are presented in Table 2. The dry unit weight after compaction were 19 kN/m^3 with a variation of $\pm$ 1.0 and the moisture content was 4% with a variation of ± 1%. Direct shear tests on this sand at density of 19 kN/m^3 and moisture content of 4% revealed peak internal friction angles of ϕ_p=52° and residual internal friction angles of ϕ_r=48°.

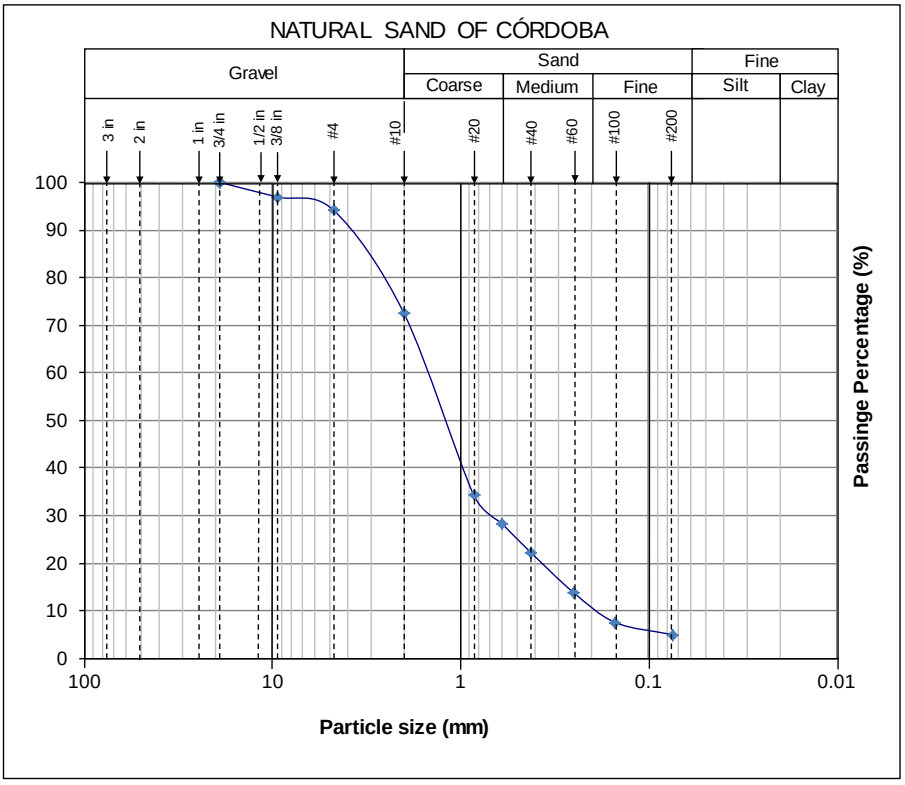

Figure 1: Granulometric distribution of the sand.

Geosynthetic

Two types of geosynthetic commercialized by CORIPA S.A, a local company were used in the experimental program. The first series of tests was carried out with the inclusion of uniaxial geogrid denominated as FORTRAC 35MP (J700). This geogrid is made of polyvinyl alcohol (PVA) yarns. The second series of tests was carried out with the inclusion of biaxial geogrid denominated as FORNIT 20 / 20 (J400). This geogrid is fabricated of polypropylene (PP) yarns. In Table 1, the mechanical strength parameters of the two types of geogrid used in the tests are shown.

Table 1: Mechanical properties of geogrids

Property	Unit	Value for Geogrid Uniaxial Fortrac 35MP (J700)	Value for Geogrid Biaxial Fornit 20/20 (J400)
Modulus (Long. Direction) (to def. 5%)	kN/m	630	≥ 360
Modulus (Cross Direction) (to def. 5%)	kN/m	-	≥ 360
Modulus (Long. Direction) (to def. 2%)	kN/m	700	≥ 400
Modulus (Cross Direction) (to def. 2%)	kN/m	-	≥ 400
Mesh opening	mm x mm	20 x 30	40 x 40

Experimental methodology

A total of 11 model tests were carried out on sand with and without geogrid included. The first test specimen without reinforcement and the others were divided into two sets of 5 samples each. The first series of tests of 5 samples was performed with the inclusion of uniaxial geogrid and the second test series of 5 samples was performed with the inclusion of biaxial geogrid. Tests on each specimen were repeated until the data is validated. The results of reinforced sand samples were compared with the results of the test sand without reinforcement in order to evaluate the improvement achieved in the stress-strain behavior of the reinforced soil mass. Schematic diagram of the test setup is shown in Figure 2, the geometric arrangement of the layers of geogrid into the soil mass is shown. The variables shown in the scheme are: distance between the base of the foundation and the first layer of geogrid (u), the number of geogrid layers (N), vertical distance between layers of geogrid (h), diameter geogrid (L) and diameter circular footing (B).

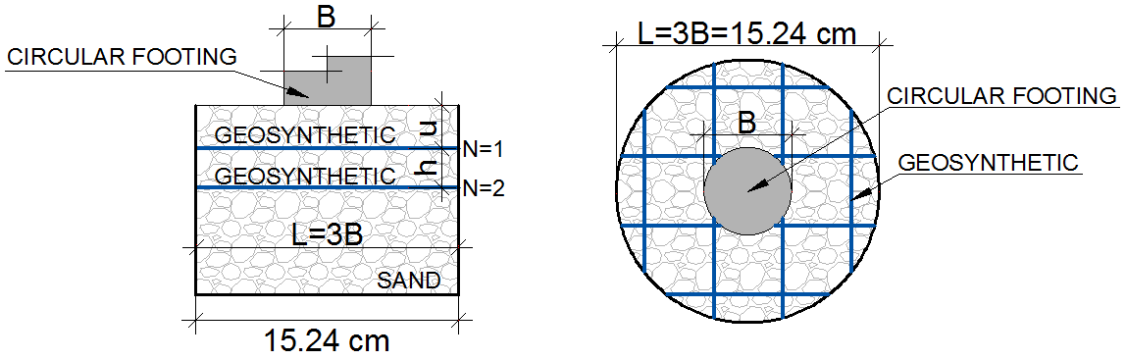

Figure 2: General model test, (a) Profile view, (b) Plant view.

The dimensions of the samples prepared for testing are shown in Figure 3. Table 2 presents the description, compaction and geometric variables of each sample prepared. The samples of the first series of tests with the uniaxial geogrid are identified with the prefix UNI and the samples of the second series of tests with the biaxial geogrid are identified with the prefix BIA. The specimen without reinforcement (Figure 3a) and the first three samples of each series of tests (Figures 3b, 3c and 3d) were prepared in a cylindrical mold of 152.4 mm in diameter and 110 mm

of height after compaction. The geogrid was cut into the circular bore size of the mold and introduced into the soil mass as the geometry shown in Figures 3b, 3c and 3d. For specimens with geogrid anchored to the edge of the mold, two rings with 152.4 mm of diameter and 53 mm of height were used in order to press the geogrid and thus restrict movement of the geogrid on the edge of the mold; for a geogrid layer halfway the sample, the height of the specimen after compaction was 106 mm (see Figure 3e) and for the sample with a geosynthetic layer on the upper third part the height of the specimen after compaction was 82 mm (see Figure 3f). Compaction of the material was using a 5.5 lb hammer (2.5 kg) with different layers according to the sample volume or the purpose of conserving constant compaction energy as can be seen in Table 2. On the samples, a surcharge of 4.5 kg was applied.

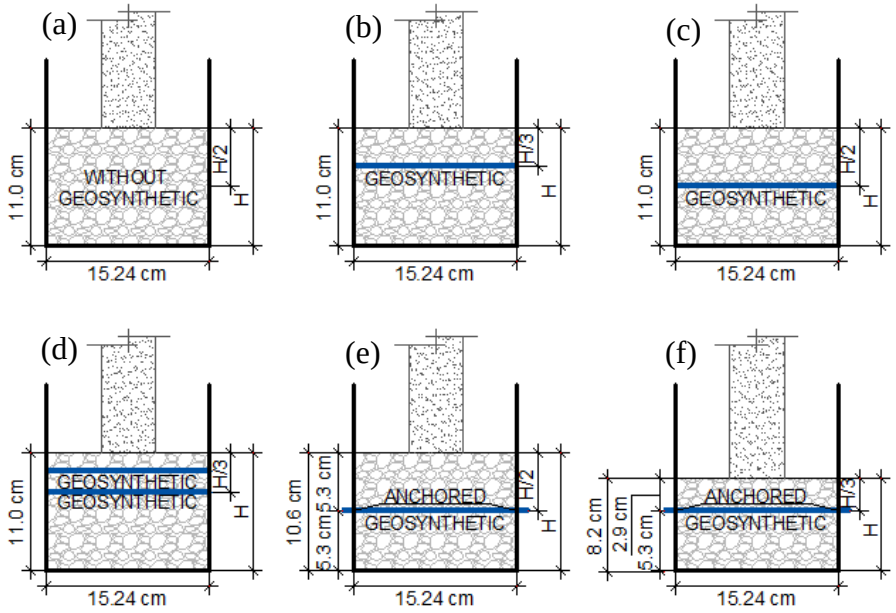

Figure 3: Scheme of the tests described in Table 2, (a) Specimen No. 1, (b) Specimens UNI-2 and BIA-2, (c) Specimens UNI-3 and BIA-3, (d) Specimens UNI-4 and BIA-4, (e) Specimens UNI-5 and BIA-5, (f) Specimens UNI-6 and BIA-6.

The rigid foundation was modeled by a circular footing made of steel with diameter B=50.8 mm and thickness greater than the diameter (t>B) enough to avoid deformation during testing. The load is applied through a press with a capacity of 50 KN. Load readings of every 0.2 mm piston settlement up to a depth of 20 mm were taken. This was followed by readings every 1 mm until completing a depth of 25 mm, where the trial ends. The load was recorded by a load cell and the settlements of the foundation were read by a digital dial. Data were acquired using a DTF Datalogger where they are passed directly to the computer for processing.

Table 2: Tests conducted.

No. Specimen	Description of the test	Compaction of the sample	u/B	h/B	L/B	N
1	Without geosynthetics	Three layers, 55 blows each	-	-	-	-
UNI-2 and BIA-2	A geosynthetic layer on the upper third part of the sample	Three layers, 55 blows each	0.6	-	3	1
UNI-3 and BIA-3	A geosynthetic layer halfway the sample	Three layers, 55 blows each	1	-	3	1
UNI-4 and BIA-4	Two layers of geosynthetics on the upper third part of the sample	Three layers, 55 blows each	0.25	0.25	3	2
UNI-5 and BIA-5	A geosynthetic layer halfway the sample anchored in the edge of the mold	Two layers 83 blows each	1	-	3	1
UNI-6 and BIA-6	A geosynthetic layer on the upper third part of the sample anchored in the edge of the mold	Three layers, 42 blows each	0.6	-	3	1

RESULTS AND DISCUSSION

Load-settlement tests

Stress - settlement curves were made with the results obtained in load tests. These curves were plotted for each specimen tested and grouped according to the type of geogrid used. Figure 4 shows the stress - settlement curves for the first series of tests with uniaxial geogrid and Figure 5 shows the stress- settlement curves for the second series of tests with biaxial geogrid, in both groups of curves results for the specimen without reinforcement are included in order to assess improvements in reinforced soil. The horizontal axis of Figures 4 and 5 shows the stress values, the primary vertical axis shows the measured values of absolute settlement and the secondary vertical axis shows the values measured of relative settlement (s/B).

As shown in Figure 4, an improvement occurs in the stress-strain behavior for specimens with uniaxial geogrid. The specimen with a geogrid layer on the upper third part of the sample anchored in the edge of the mold (UNI-6) presented the best behavior together with the specimen with two layers of geogrid on the upper third part of the sample (UNI-4). Moreover, the specimen with a geogrid layer halfway the sample (UNI-3) did not show any improvement except when the geogrid is anchored to the mold (UNI-5), where the specimen presented an improvement similar to that obtained with the specimen (UNI-2) with a geogrid layer on the upper third part of the sample. Stress- settlement results obtained for the samples with biaxial geogrid are presented in Figure 5. In this case, the specimen with a geogrid layer halfway the sample (BIA-3) presented improvement in contrast to the same test specimen with uniaxial geogrid included (UNI-3). The behavior of the other samples is similar to the specimens with uniaxial geogrid, the specimen with a geogrid layer halfway the sample anchored in the edge of the mold (BIA-5) shows a similar improvement to the specimen (BIA-2) with a geogrid layer halfway the sample anchored in the edge of the mold. The best results were obtained for the specimen with two layers of geogrid on the upper third part of the sample (BIA-4), and for the specimen with a geogrid layer on the upper third part of the sample anchored in the edge of the mold (BIA-6).

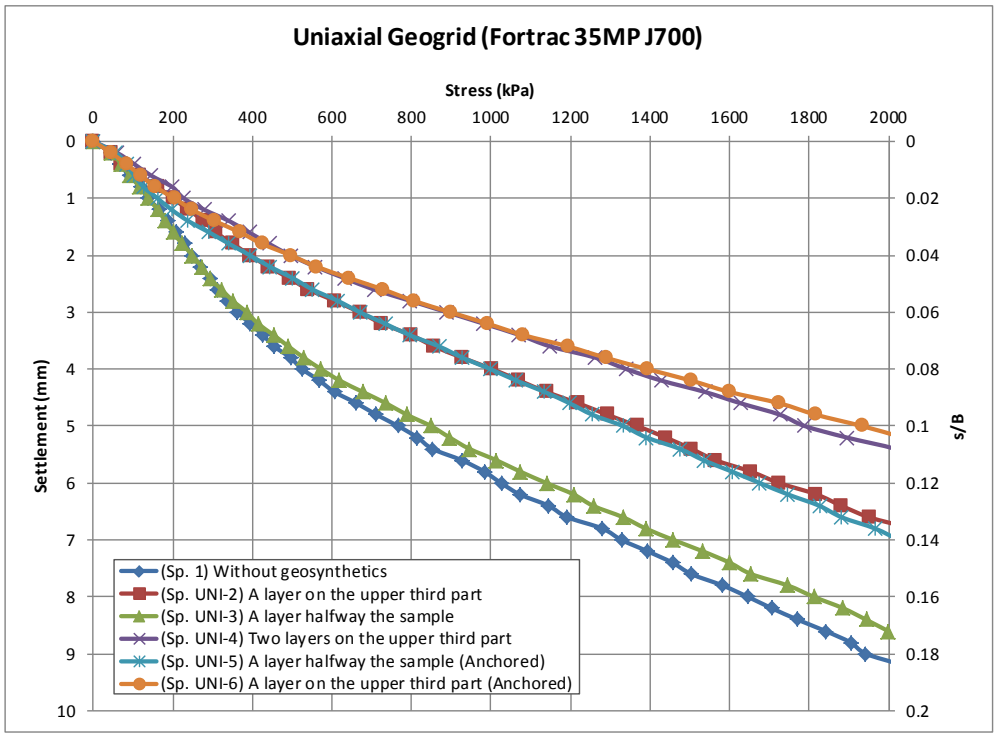

Figure 4: Stress vs. Settlement for the specimens tested with uniaxial geogrid.

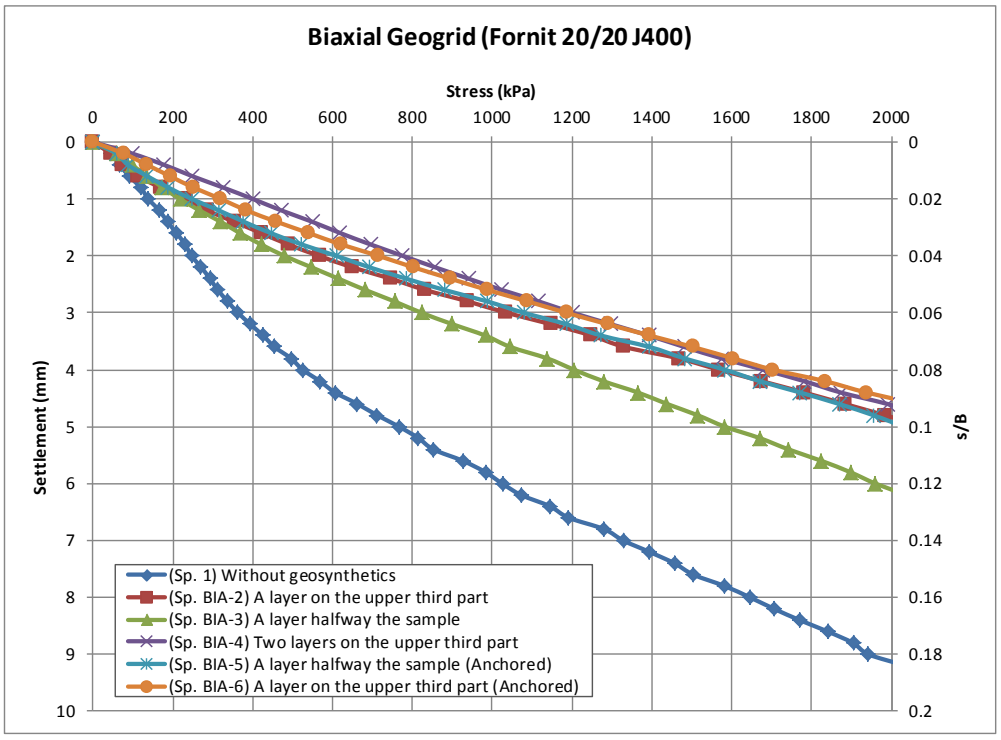

Figure 5: Stress vs. Settlement for the specimens tested with biaxial geogrid.

Bearing capacity behavior

In order to estimate the improvement of the soil produced by the inclusion of geogrids, the BCR (Bearing Capacity Ratio) is calculated for each of the samples tested. In this paper, the Bearing Capacity Ratio for the same settlement (BCR_s) is calculated. This value is calculated for each value of measured load and is defined as:

$$BCR_s = \frac{q_{(R)}}{q_{(U)}} \quad (1)$$

where $q_{(U)}$ and $q_{(R)}$ are load-bearing capacity values for unreinforced and reinforced foundations, respectively, at the same settlement (Latha and Somwanshi 2009). BCR_s values against relative settlement (s/B) for each of the samples are plotted in Figures 8, 11, 14 and 15.

Stress Ratio Index (SR)

In order to verify the improvement in reinforced soil produced at low strains was calculated the Stress Ratio Index (SR), this index relates the stress values obtained in load tests with standard values to the same deformation. It was calculated for each specimen as follows:

$$SR = \frac{\text{Stress (kPa)}}{\text{Standard Stress (kPa)}} * 100 \quad (2)$$

This index is calculated for stress values corresponding to 2.5 mm and 5.0 mm of settlement obtained from stress-settlement curves (Figure 4 and Figure 5), which are divided between CBR test standard stress of 1000 Psi (6900 kPa) and 1500 psi (10300 kPa) respectively. Figure 6 presents SR values for all samples.

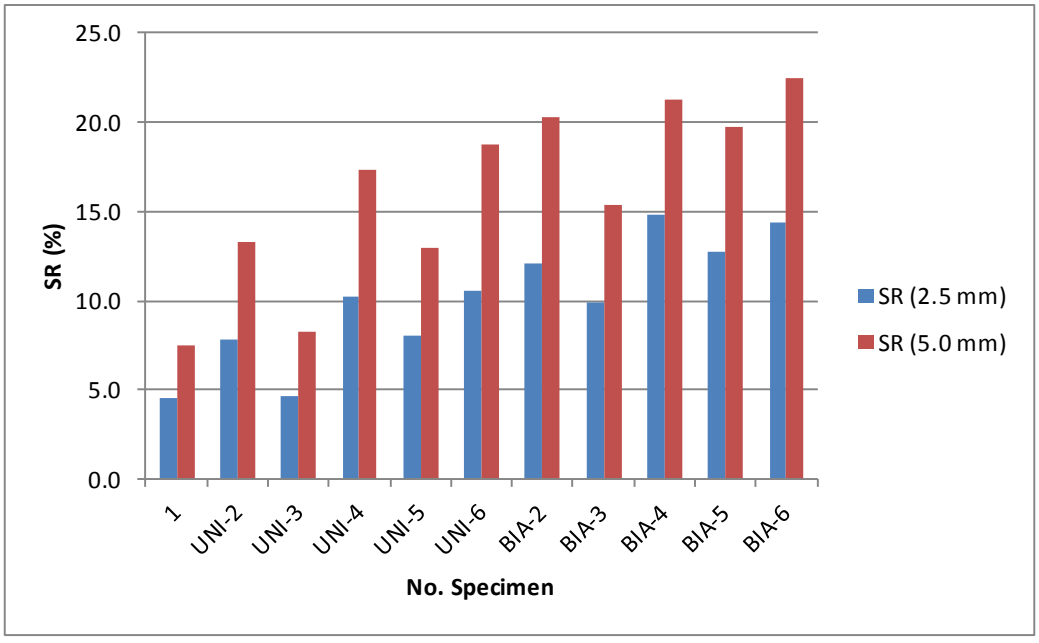

Figure 6: SR for the specimens tested.

Geogrid vertical displacement

Vertical relative deformations in the geogrid were measured for each of the samples tested. These measurements were made from the upper horizontal plane of the specimen, every 2 cm from the central axis considering the directions shown in Figure 7. Before measuring, the soil above the layer of geosynthetic in the specimen was removed. Vertical profiles were performed along the coordinate axes for each layer of geosgrid, obtaining the resulting deformation in the geogrid at the end of the test. The results of these measurements show some small initial deformations caused by soil compaction, these are located at different points of geogrid and are most evident in the samples in which the geogrid is not anchored to the mold. The vertical relative displacements in the geogrid layers along the x-axis for the different samples are shown in Figures 9, 12 and 16. The vertical relative displacements in the geogrid layers along the y-axis for the different samples are shown in Figures 10, 13 and 17.

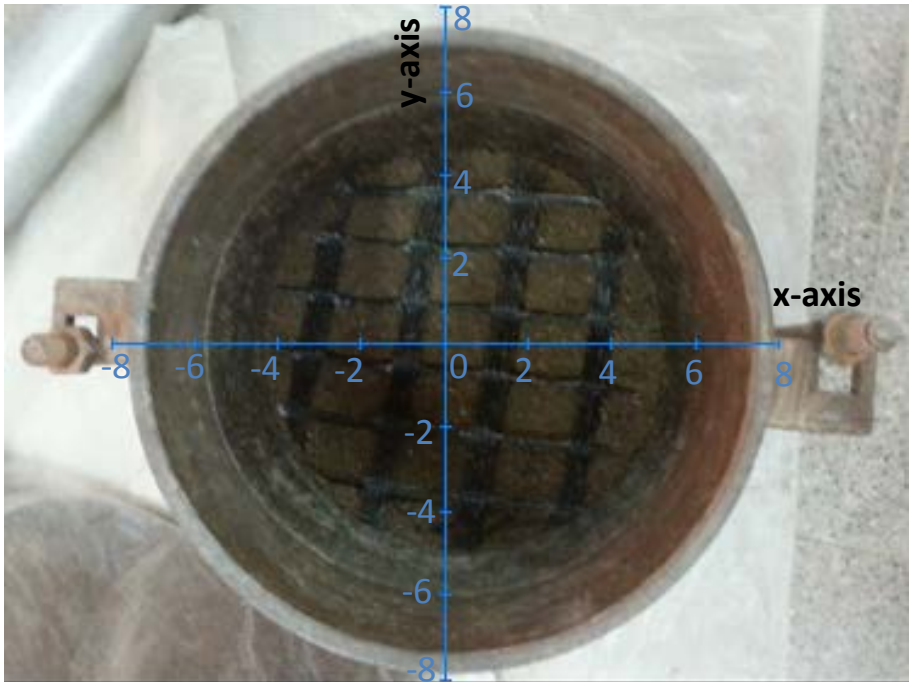

Figure 7: Axes (Unit: cm) used to measure the vertical displacements in the geogrid.

Variables analysis

In this section is established the relationship between stress-strain behavior of the soil and the different geogrid variables including the effect of number of geogrid layers (N), distance between the base of the foundation and the first layer of geogrid (u), the effect when the geogrid is anchored in the edge to the test mold and type of geogrid reinforcement used. The analysis was performed with BCR_s vs. (s/B) graphs, calculated values of SR Index and measures the vertical deformations in the geogrid layers after completion of the test. These results are discussed following.

Effect of number of reinforcing layers

To evaluate this variable, the results of the specimens with a geogrid layer on the upper third part of the sample (UNI-2 and BIA-2) are compared with the results of the specimens with two layers of geogrids on the upper third part of the sample (UNI-4 and BIA-4). Figure 8 shows the graph of BCR_s vs. (s/B) for the specimens with one and two layers of geogrid on the upper third part of the sample for both types of geogrid (UNI-2, UNI-4, BIA-2 and BIA-4). As shown in Figure 8, the behavior of these curves shows that improved by including a second layer is more significant when the uniaxial geogrid is used and more moderate when biaxial geogrid is used. The maximum value for BCR_s changes from 1.9 to 2.6 when a second layer of uniaxial geogrid is included. This value changes from 3.0 to 3.3 when a second layer of biaxial geogrid is included. An increase of 0.7 to uniaxial geogrid occurs while the increase is 0.3 for biaxial geogrid.

The SR index for these samples (see Figure 6) showed an increase of 2.4% for the SR (2.5 mm) and 4.1% for the SR (5.0 mm) when a second layer of uniaxial geogrid is included on the upper third part of the sample. These same indexes for biaxial geogrid samples show an increase of 2.8% for the SR (2.5 mm) and 1.0% for the SR (5.0 mm) when a second layer of biaxial geogrid is included on the upper third part of the sample. Which confirms that the improvement produced by a second layer is more moderate when used biaxial geogrid. Figures 9 and 10 compare deformations in the geogrid after the trial for specimens with one and two layers of geogrid on the upper third part of the sample (UNI-2, UNI-4, BIA-2 and BIA-4). The graphs show that the greatest deformations occurring in the top layer of the specimens with two layers of geogrid on the upper third part of the sample (UNI-4 and BIA-4). Deformations in the bottom layer of the specimens UNI-4 and BIA-4 showed similar results to the specimens UNI-2 and BIA-2 with a geogrid layer on the upper third part of the sample. In the consulted research is reported that the optimal number of geosynthetic varies between three or four layers, this should be checked with a larger scale trial.

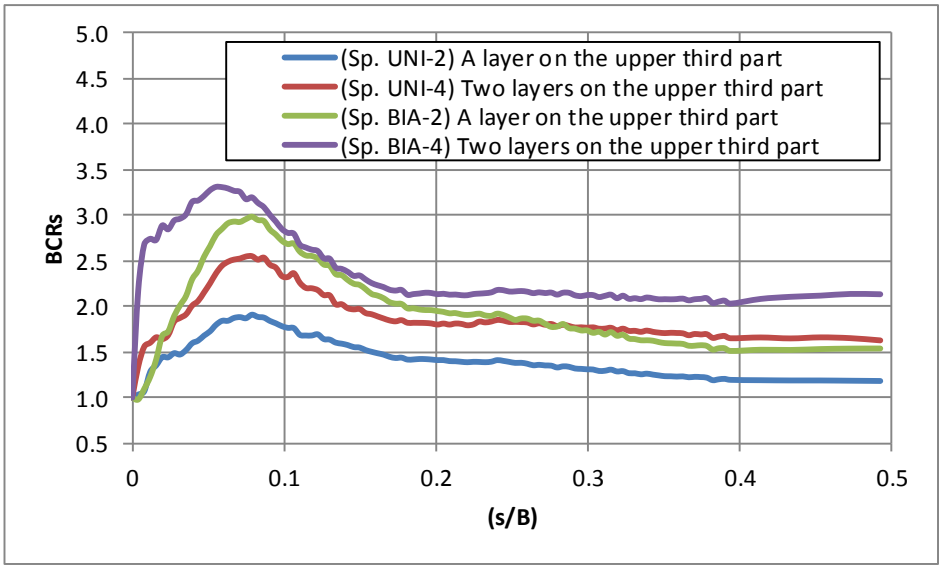

Figure 8: Variations of BCRs with (S/B) for different N.

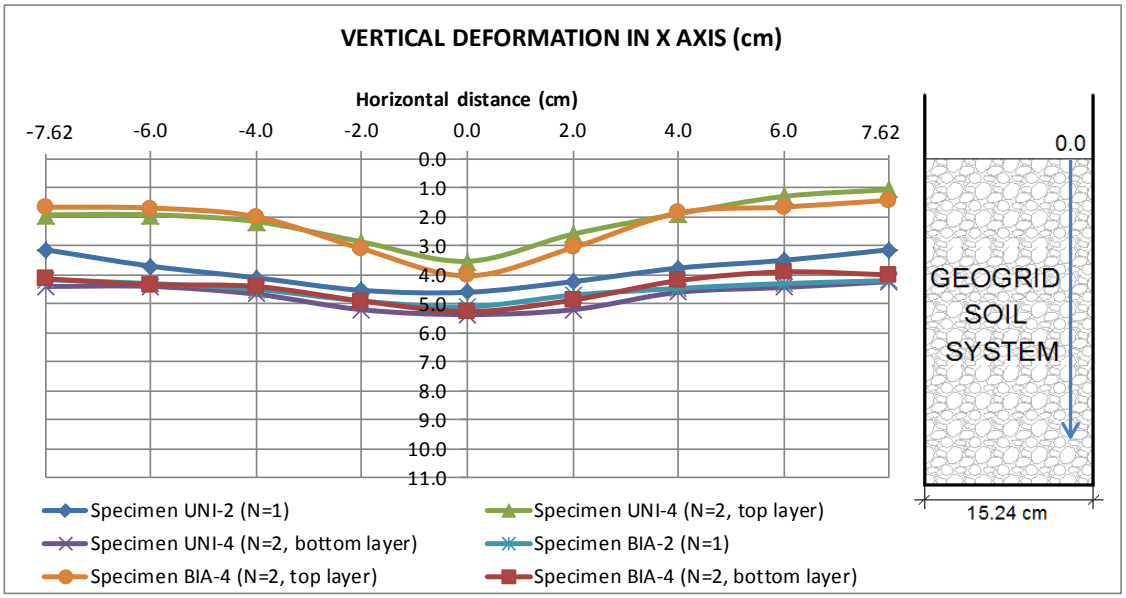

Figure 9: Geogrid vertical displacement (x-axis) for different N.

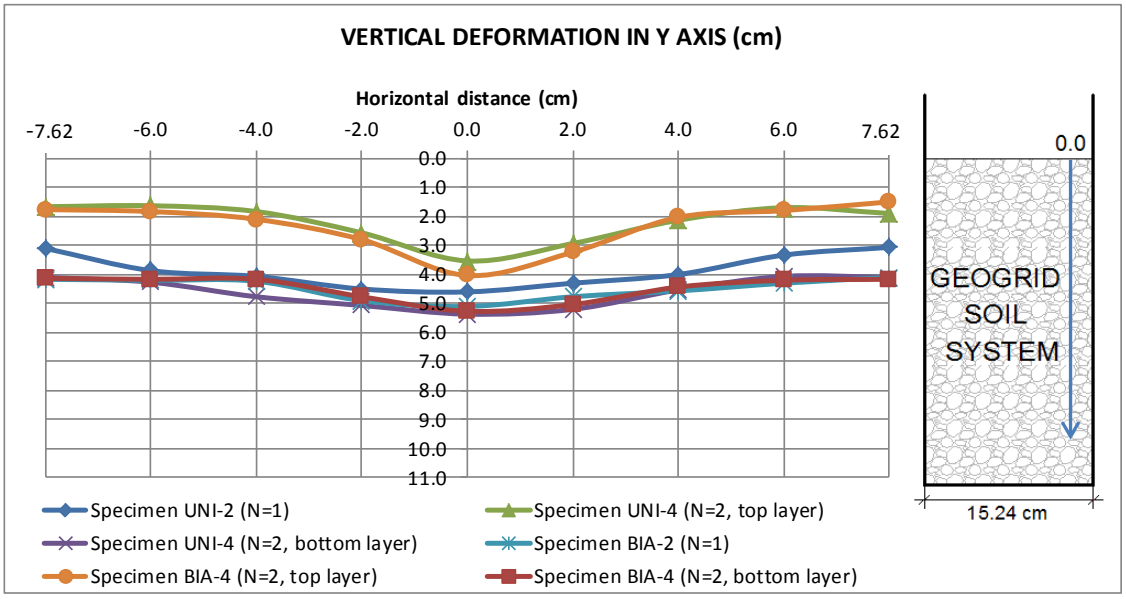

Figure 10: Geogrid vertical displacement (y-axis) for different N.

Effect of depth to top layer

The effect of the vertical distance between the base of the foundation and the first layer of geogrid (u), is studied with the results of the specimens with a geogrid layer on the upper third part of the sample (UNI-2 and BIA-2) which have a value (u/B=0.6), and the results of the specimens with a geogrid layer halfway the sample (UNI-3 and BIA-3) which have a value (u/B=1.0). In Figure 11, the graphs of BCR_s vs. (s/B) for the specimens (UNI-2, BIA-2, UNI-3 and BIA-3) are presented. The BCR_s decreases with increasing vertical distance between the base of the foundation and the first layer of geogrid. The SR index for these samples (see Figure 6) also they show a decreasing behavior with increasing vertical distance between the base of the foundation and the first layer of geogrid. In Figures 12 and 13, the final displacements of the

geogrid obtained for these specimens are compared. Vertical deformations in specimens with (u/B=0.6) are much greater than deformations in specimens with (u/B=1.0) for both types of geogrid.

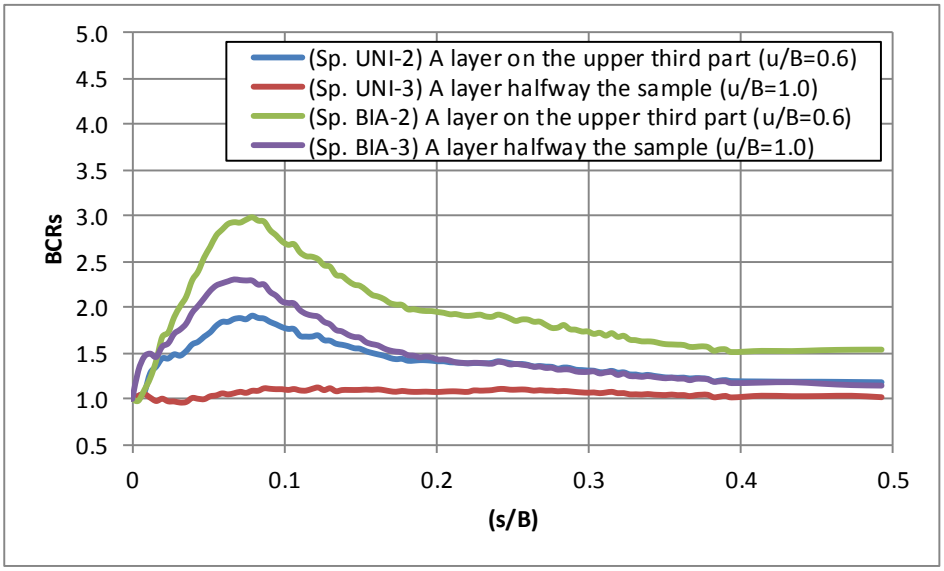

Figure 11: Variations of BCRs with (S/B) for different depth of geogrid layer (u/B).

.

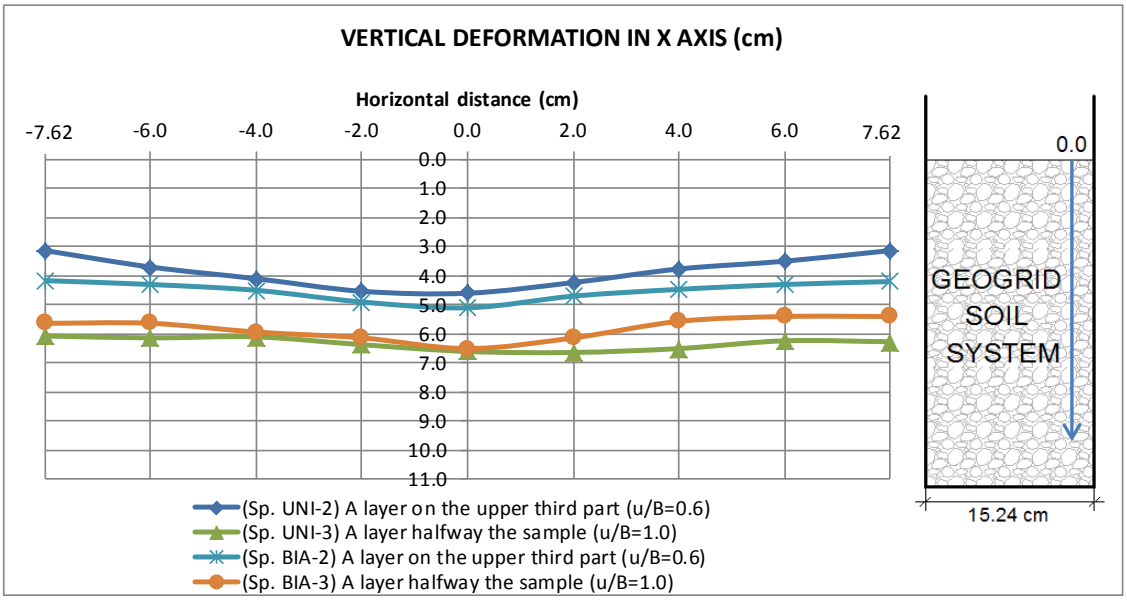

Figure 12: Geogrid vertical displacement (x-axis) for different depth of geogrid layer (u/B).

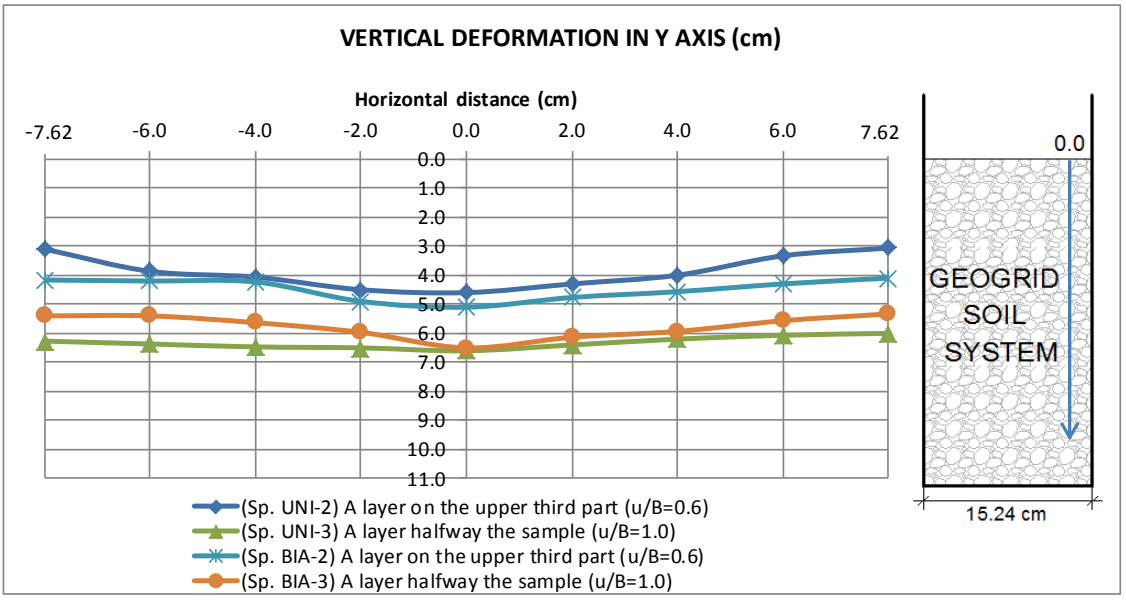

Figure 13: Geogrid vertical displacement (y-axis) for different depth of geogrid layer (u/B).

Effect of geogrid anchored to the test mold

To establish the effect of geogrid anchored to the test mold, the results of the specimens with a geogrid layer on the upper third part of the sample (UNI-2 and BIA-2) and the results of the specimens with a geosynthetic layer on the upper third part of the sample anchored in the edge of the mold (UNI-6 and BIA-6) are compared. Also the results of the specimens with a geogrid layer halfway the sample (UNI-3 and BIA-3) and the results of the specimens with geogrid layer halfway the sample anchored in the edge of the mold (UNI-5 and BIA-5) are compared. Figures 14 and 15, shows the graphs of BCR_s vs. (s/B) for geogrid unanchored and anchored to the test mold. These curves show the increase produced in BCR_s when the geogrid layers are anchored to the test mold. Improving produced in the soil is more significant when the uniaxial geogrid is used and more moderate when biaxial geogrid is used.

A similar increase in the stress-strain behavior can be seen for small deformations, when SR index values for these specimens are compared (see Figure 6). The effect of anchored for the specimens with a geogrid layer on the upper third part of the sample shows that SR index (2.5 mm) increases 2.7% when uniaxial geogrid is used (UNI-2 and UNI-6) and increases 2.3% when biaxial geogrid is used (BIA-2 and BIA-6). Likewise, SR index (5.0 mm) increases 5.5% when uniaxial geogrid is used and increases 2.3% when biaxial geogrid is used. For the specimens with a geogrid layer halfway the sample SR index (2.5 mm) increases 3.3% when uniaxial geogrid is used (UNI-3 and UNI-5) and increases 2.9% when biaxial geogrid is used (BIA-3 and BIA-5). Likewise, SR index (5.0 mm) increases 4.7% when uniaxial geogrid is used and increases 4.4% when biaxial geogrid is used. Figures 16 and 17 compare deformations in the geogrid after the trial for unanchored and anchored samples. The graphs show that the anchored samples have higher deformations, which indicates that the tension force developed by the geogrid anchored to the mold is greater than that developed by the geogrid unanchored to the mold.

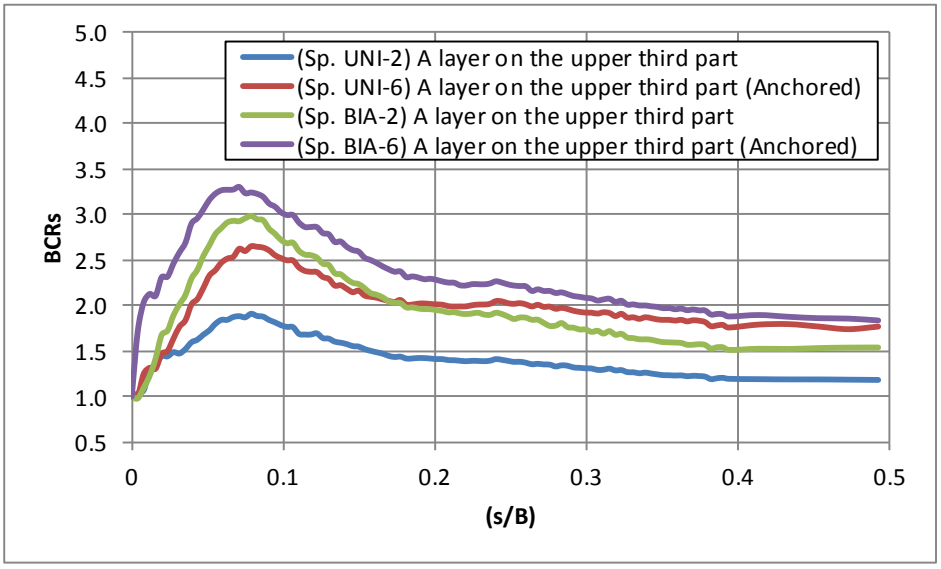

Figure 14: Variations of BCRs with (S/B) for geogrid unanchored and anchored for specimens with a geogrid layer on the upper third part of the sample.

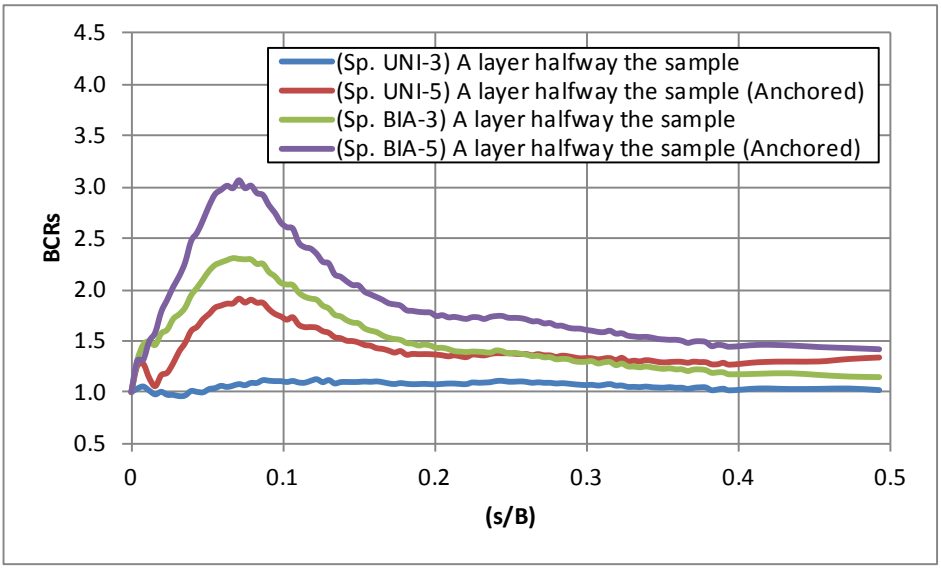

Figure 15: Variations of BCRs with (S/B) for geogrid unanchored and anchored for specimens with a geogrid layer halfway of the sample.

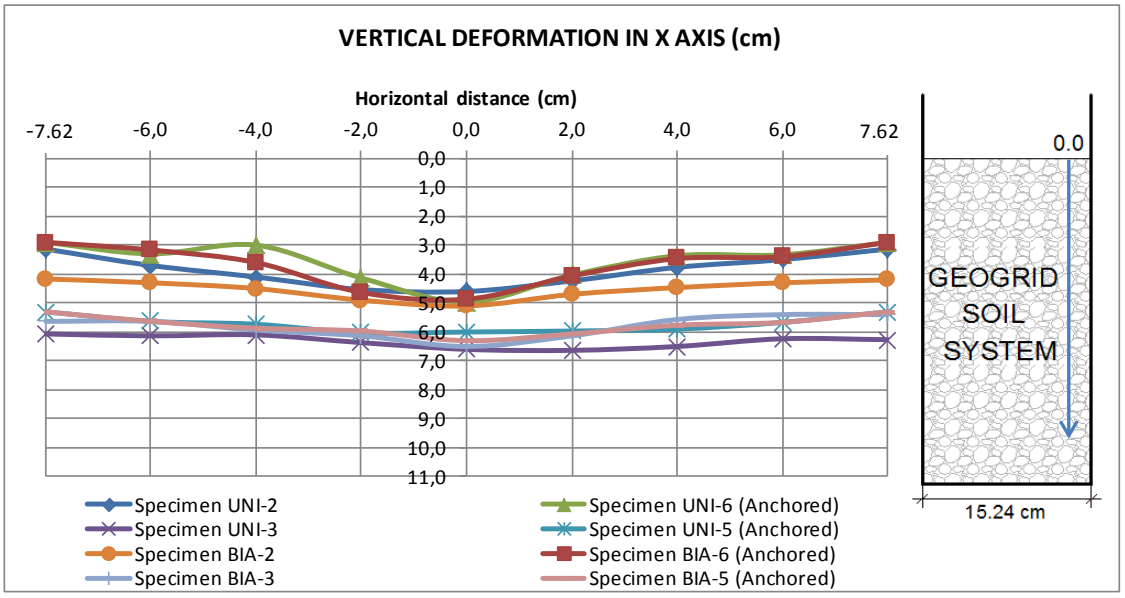

Figure 16: Geogrid vertical displacement (x-axis) for geogrid unanchored and anchored.

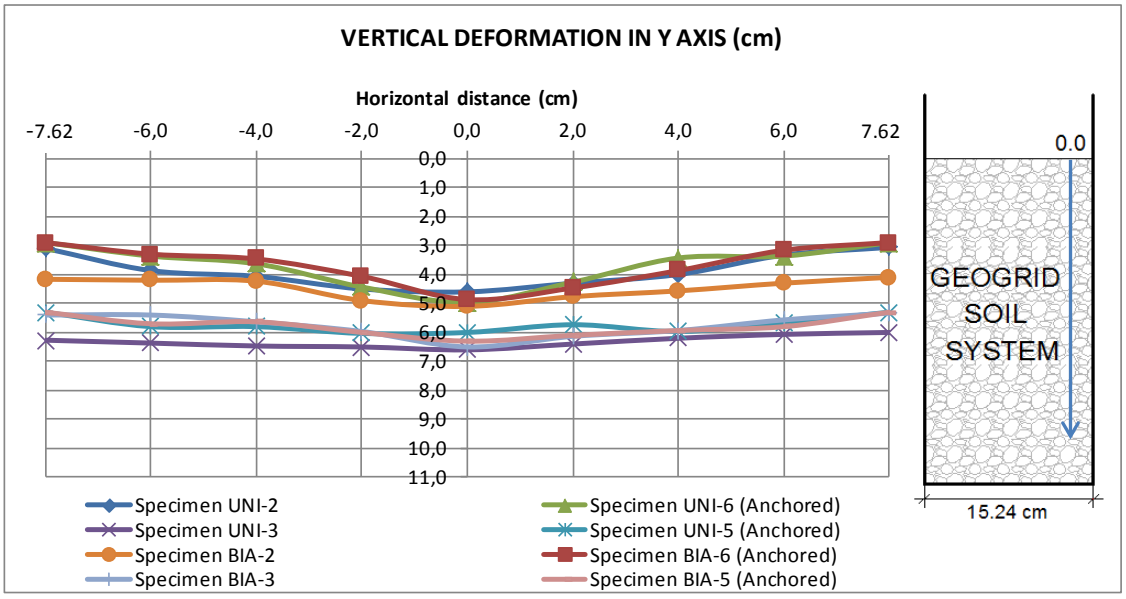

Figure 17: Geogrid vertical displacement (y-axis) for geogrid unanchored and anchored.

Results according to the geogrid used

Figures 8, 11, 14 and 15 presents the results obtained from the analysis of BCR_s, the values are greater for samples with biaxial geogrid. The calculated values for SR index also showed greater increases for samples prepared with biaxial geogrid (see Figure 6). An important result shows as for the specimens with a geogrid layer halfway the sample (UNI-3 and BIA-3), increase seen in bearing capacity using biaxial geogrid (BIA-3) while using uniaxial geogrid (UNI-3) that no increase occurs in the bearing capacity. Figures 9, 10, 12, 13, 16 and 17 shows vertical relative deformations in the geogrid at the end of the test, these values show that both types of geogrid are deformed similarly.

Scale effects

It is well recognized that small-scale model test studies carried out in granular soils involve a scale error. In the present study, the model tests were conducted on a small-scale model footing, while the used sand and geogrids were the same dimensions as in the field. Therefore, model footing or the soil may not play the same role as in the field and it might cause some influence on the model test results. The scale of the trials does not allow a broader study of the variable geometry of the geogrid in the soil mass. To incorporate more layers of geogrid to the soil samples and perform a wide and controlled variation of the variables studied here, scale experiments will increase. The results obtained with the geogrid anchored to mold test indicate the need to establish a sufficient anchorage length in geogrid, this length may be determined with larger scale trials. To scale up testing will also be possible to study variables such as soil particle size, foundation depth, the size of the geogrid layer, vertical distance between layers of geosynthetic and the shape and dimensions of the foundation.

CONCLUSIONS

The bearing capacity behavior of a circular footing resting on the reinforced-sand was investigated experimentally. Results obtained from the present investigation showed a significant increase in the bearing capacity of the soil and reduced settlement in the foundation. Following conclusions may be drawn from the present study:

1. Laboratory tests showed that by including biaxial geogrid in the soil mass, produced a greater increase in the bearing capacity that by including uniaxial geogrid. This happens because the biaxial geogrid can withstand tensions in both directions, so the pressures on the ground are distributed more symmetrically. For circular foundations biaxial geogrids performs better, which can be caused by the symmetry of the foundation. Would be important to evaluate the behavior of this type of geogrids to strip foundations that do not present the symmetry in all directions of the circular foundations.

2. Vertical distance between the base of the foundation and the first layer of geogrid has direct influence on the improvement produced in the reinforced-sand. In this case it was established that best results are achieved when this distance is (u = 0.6 B) that when (u = 1.0 B). Tests must be performed on a large-scale for a broader evaluation and establish the optimal value of this variable.

3. The number of layers of geogrid in the sample has an effect on the values of bearing capacity and settlement of circular foundation. In this case, the improvement produced by the inclusion of a second layer in the soil mass was most marked in the samples prepared with uniaxial geogrid, these samples showed a linear growth in bearing capacity when it is passed from one layer to two layers of geogrid. For samples with biaxial geogrid the increase was more moderate but evident.

4. The improvement obtained when the geogrid layer is boundary anchored by the mold, is better than when it is left unanchored. The tension force developed by the geogrid when it is anchored to the mold can clearly be seen, therefore it is important to establish a sufficient length in geosynthetic, enough to ensure that this force occurs. In the present tests, a size of geogrid three times the width of the foundation (3B) was used. It should determine the optimum length of geogrid with larger scale trials.

5. The BCR_s shows a peak value in all curves to relating settlements (s/B=0.08), namely for around 4mm settlements. The behavior of BCR_s vs. (s/B) presents a curve with two differentiated zones denominated as pre-peak and post-peak. It is estimated that this can

be provisionally explained as follows: (1) First, the development of tension in the geosynthetic, and friction interaction sand-geogrid, during the first settlements produces an increased in modified BCR reaching a maximum at optimum combination between compacted soil and geosynthetic effect, (2) then the curve drops to stabilize at a given value of BCR, higher than one (asymptote) where, possibly, have been reaching a residual friction interaction sand-geogrid. However, it will be necessary to increase the experimental study and numerical analysis of the behavior, in order to confirm this explanation. For this, direct shear tests and large scale laboratory tests are planning, where sand-geogrid interaction can be studied.

ACKNOWLEDGMENTS

The authors would like to thank the National Scientific and Technical Research Council (CONICET), the National Technological University (UTN), the Regional Faculty of Córdoba (Argentina) and CORIPA S.A. for the geogrid samples provided.

REFERENCES

1. Abu-Farsakh, M., Chen, Q. and Sharma, R. (2013). “An Experimental Evaluation of the Behaviour of Footings on Geosynthetic-Reinforced Sand”. Soils and Foundations, the Japanese Geotechnical Society. 53(2), pp. 335-348.
2. Adams, M.T. and Collin, J.G. (1997) "Large Model Spread Footing Load Tests on Geosynthetic. Reinforced Soil Foundations", Journal of Geotechnical and Geoenvironmental Engineering, 123 (1), pp. 66-72.
3. Alawaji, H.A. (2001). “Settlement and Bearing Capacity of Geogrid-Reinforced Sand over Collapsible Soil”. Geotextiles and Geomembranes. 19, pp. 75-88.
4. Azzam, W.R. and Nasr A.M. (2014). “Bearing Capacity of Shell Strip Footing on Reinforced Sand”. Journal of Advanced Research. 1, pp. 1-11.
5. Basudhar, P.K., Saha, S. and Deb, K. (2007). “Circular Footings Resting on Geotextile-Reinforced Sand Bed”. Geotextiles and Geomembranes. 25, pp. 377-384.
6. Bergado, D.T., Youwai, S., Hai C.N. and Voottipruex, P. (2001). “Interaction of Nonwoven Needle-Punched Geotextiles under Axisymmetric Loading Conditions”. Geotextiles and Geomembranes. 19, pp. 299-328.
7. Das, B.M., Maji, A. and Shin, E.C. (1998). “Foundation on Geogrid-Reinforced Sand - Effect of Transient Loading”. Geotextiles and Geomembranes. 16, pp. 151-160.
8. DeMerchant, M.R., Valsangkar A.J. and Schriver A.B. (2002). “Plate Load Tests on Geogrid-Reinforced Expanded Shale Lightweight Aggregate”. Geotextiles and Geomembranes. 20, pp. 173-190.
9. Dixit, M.S. and Patil D.K. (2014). “Effect of Reinforcement on Bearing Capacity and Settlement of Sand”. Electronic Journal of Geotechnical Engineering (EJGE). 19, pp. 1033-1046. Available at ejge.com.
10. Duncan-Williams, E. and Attoh-Okine, N. O. (2008). “Efect of Geogrid in Granular Base Strength - An Experimental Investigation”. Journal of Construction and Building Materials. 22, pp. 2180-2184.

11. Kotake, N., Tatsuoka, F., Tanaka, T., Siddiquee, M.S.A. and Huang, C.C. (2001). “FEM Simulation of the Bearing Capacity of Level Reinforced Sand Ground Subjected to Footing Load”. Geosynthetics International. 8(6), pp. 501-549.

12. Latha, G.M. and Somwanshi, A. (2009). “Bearing Capacity of Square Footings on Geosynthetic Reinforced Sand”. Geotextiles and Geomembranes. 27, pp. 281-294.

13. Marto, A., Oghabi, M. and Eisazadeh, A. (2013). “The Effect of Geogrid Reinforcement on Bearing Capacity Properties of Soil under Static Load; A Review”. Electronic Journal of Geotechnical Engineering (EJGE). 18, pp. 1881-1898.

14. Moghaddas Tafreshi, S.N. and Dawson, A.R. (2012). “A Comparison of Static and Cyclic Loading Responses of Foundations on Geocell-Reinforced Sand”. Geotextiles and Geomembranes. 32, pp. 55-68.

15. Naeini, S.A. and Mirzakhanlari, N. (2008). “The Effect of Geotextile and Grading on the Bearing Ratio of Granular Soils”. Electronic Journal of Geotechnical Engineering. 13, pp. 1-10. Available at ejge.com.

16. Phanikumar, B.R., Prasad, R. and Singh, A. (2009). “Compressive Load Response of Geogrid-Reinforced Fine, Médium and Coarse Sands”. Geotextiles and Geomembranes. 27, pp. 183-186.

17. Patra, C.R., Das, B.M. and Atalar, C. (2005). “Bearing Capacity of Embedded Strip Foundation on Geogrid-Reinforced Sand”. Geotextiles and Geomembranes. 23, pp. 454-462.

18. Senthil Kumar, P. and Rajkumar, R. (2012). “Effect of Geotextile on CBR Strength of Unpaved Road with Soft Subgrade”. Electronic Journal of Geotechnical Engineering. 17, pp. 1355-1363. Available at ejge.com.

19. Useche Infante, D.J., Aiassa Martinez, G., Arrúa, P. and Eberhardt, M. (2015). “Stress-Strain Behavior of Geosynthetic Reinforced Soil Using a Modified CBR Test”. Fifth International Conference on Geotechnique, Construction Materials and Environment, Osaka, Japan, Nov. 16-18, 2015.

20. Wasti, Y. and bütün, M.D. (1996). “Behaviour of Model Footings on Sand Reinforced with Discrete Inclusions”. Geotextiles and Geomembranes. 14, pp. 575-584.

21. Yadu, L. and Tripathi, R.K. (2013). “Effect of the Length of Geogrid Layers in the Bearing Capacity Ratio of Geogrid Reinforced Granular Fill-Soft Subgrade Soil System”. Procedia - Social and Behavioral Sciences. 104, pp. 225-234.

22. Yetimoglu, T., Inanir, M. and Inanir, O. (2005). “A Study on Bearing Capacity of Randomly Distributed Fiber-Reinforced Sand Fills Overlying Soft Clay”. Geotextiles and Geomembranes 23, pp. 174–183.